

Measurements of Unitarity-Triangle Sides: Semileptonic B-Meson Decays

Jochen Dingfelder^{*†}

Universität Freiburg

E-mail: jdingfel@cern.ch

We present the status of determinations of the Cabibbo-Kobayashi-Maskawa matrix elements $|V_{cb}|$ and $|V_{ub}|$, whose ratio $|V_{ub}|/|V_{cb}|$ is proportional to the side of the Unitarity Triangle opposite to the angle β . Recent measurements of inclusive and exclusive semileptonic B -meson decays with charm, $B \rightarrow X_c \ell \nu$, and without charm, $B \rightarrow X_u \ell \nu$, at the B factories are discussed.

*12th International Conference on B-Physics at Hadron Machines
September 7-11, 2009
Heidelberg, Germany.*

^{*}Speaker.

[†]for the BaBar and Belle Collaborations

1. Introduction

The elements of the Cabibbo-Kobayashi-Maskawa (CKM) quark-mixing matrix are fundamental parameters of the Standard Model. Precise determinations of the magnitudes of the CKM matrix elements V_{cb} and V_{ub} are important tests of the flavor sector of the Standard Model. They complement the measurements of CP asymmetries in B -meson decays, in particular $\sin 2\beta$, and thus provide stringent tests of the Standard Model mechanism for CP violation. One of the unitarity conditions of the CKM matrix can be graphically represented as a triangle, the Unitarity Triangle. The ratio $|V_{ub}|/|V_{cb}|$ is proportional to the length of its side opposite to the well-measured angle β . The values of $|V_{cb}|$ and $|V_{ub}|$ can be extracted from measurements of semileptonic B -meson decays. A comprehensive review of semileptonic B decays and the determination of Unitarity-Triangle sides is beyond the scope of these proceedings. In the following the current status of $|V_{cb}|$ and $|V_{ub}|$ determinations is presented with a focus on the most recent measurements at the B factories.

2. Semileptonic B Decays and Experimental Methods

The BaBar and Belle experiments have collected large samples of several hundred millions of $B\bar{B}$ pairs from e^+e^- collisions at the $\Upsilon(4S)$ resonance. The cleanest way to determine the CKM matrix elements $|V_{cb}|$ and $|V_{ub}|$ is by measuring semileptonic B -meson decays $B \rightarrow X_c \ell \nu$ and $B \rightarrow X_u \ell \nu$, respectively. For these decays, the leptonic and hadronic components of the matrix element factorize. The measurements can be performed with inclusive or exclusive decays. The experimental and theoretical uncertainties of the two approaches are different and largely independent, thus providing important cross-checks of our understanding of theory and measurements.

Different ‘‘tagging’’ techniques are used which differ in the way the second B meson in the $B\bar{B}$ event is treated. In untagged analyses, the second B meson is not explicitly reconstructed. The four-momentum of the neutrino from the semileptonic decay must be inferred from the difference between the sum of the colliding-beam four-momenta and the total four-momentum measured in the event. Untagged analyses yield the largest signal samples, but suffer from large backgrounds. In tagged analyses, one of the two B mesons is either partially or fully reconstructed. In the hadronic-tag technique, one B meson is fully reconstructed in a hadronic decay ($B_{tag} \rightarrow D^{(*)}Y$, where Y denotes a combination of $\pi^{0,\pm}$ and $K^{0,\pm}$). Thus the event kinematics are fully constrained, the four-momentum as well as the charge and flavor of both B mesons are known and combinatorial backgrounds are basically eliminated. However, the tagging efficiency is only of the order of 10^{-3} .

3. Inclusive $B \rightarrow X_c \ell \nu$ Decays and $|V_{cb}|$

Inclusive determinations of $|V_{cb}|$ rely on calculations of the semileptonic B decay rate within the framework of Operator Product Expansions (OPE). The total decay rate is given by

$$\Gamma(B \rightarrow X_c \ell \nu) = \frac{G_F^3 m_b^5}{192 \pi^3} |V_{cb}|^2 (1 + A_{ew}) A_{pert} F(r, \frac{\mu_\pi^2}{m_b^2}, \frac{\mu_G^2}{m_b^2}, \frac{\rho_D^3}{m_b^3}, \frac{\rho_{LS}^3}{m_b^3}, \dots), \quad (3.1)$$

where $r = m_c/m_b$, A_{ew} and A_{pert} denote electroweak and perturbative QCD corrections, and the term F is written as an expansion in powers of $1/m_b$ and depends on a set of non-perturbative parameters ($\mu_\pi, \mu_G, \rho_D, \rho_{LS}, \dots$). The expression is known up to $1/m_b^4$.

The non-perturbative parameters must be determined from inclusive observables such as moments of kinematic distributions, e.g. lepton-energy or hadron-mass spectra in $B \rightarrow X_c \ell \nu$ decays or photon-energy spectrum in $B \rightarrow X_s \gamma$ decays. Moment measurements have been performed by CLEO, BaBar, Belle, DELPHI, and CDF (see webpage of the Heavy Flavor Averaging Group (HFAG) [1] for more information and references). Calculations of the decay rate and moments exist in two schemes, the kinetic [2] and the $1S$ [3] schemes, referring to the b -quark mass definition.

The large data samples recorded by BaBar and Belle can provide clean samples of events with a tagged B meson. In inclusive $B \rightarrow X_c \ell \nu$ analyses, the B_{tag} is fully reconstructed and the lepton ($\ell = e$ or μ) from the signal B decay is identified. The consistency of the B_{tag} with a B meson is tested using the variables $m_{ES} = \sqrt{s/4 - \vec{p}_B^2}$, the energy-substituted B mass, and $\Delta E = E_B - \sqrt{s}/2$, the difference between the reconstructed and expected B energies, where E_B and \vec{p}_B are the energy and the momentum of the B_{tag} in the $Y(4S)$ rest frame and \sqrt{s} is the center-of-mass energy. All particles not used in the reconstruction of the B_{tag} or identified as lepton are assigned to the hadronic system X_c , thus allowing a reconstruction of the mass of the final-state hadron, m_X , with good resolution.

BaBar has recently updated their measurement of hadron-mass moments in $B \rightarrow X_c \ell \nu$ decays [4]. Results based on a data sample of 232×10^6 $B\bar{B}$ pairs are obtained for the moments $\langle m_X^n \rangle$ ($n = 1, \dots, 6$) as a function of the lower limit on the lepton momentum in the $Y(4S)$ rest frame, $0.8 < p_{\ell, min}^* < 1.9$ GeV. These moments are affected by acceptance and resolution effects; an event-by-event correction is performed using calibration curves obtained from simulation. In this analysis, also combined hadron "mass-and-energy" moments, $\langle n_X^n \rangle$ ($n = 2, 4, 6$) with $n_X^2 = m_X^2 - 2\tilde{\Lambda}E_X + \tilde{\Lambda}^2$ and $\tilde{\Lambda} = 0.65$ GeV, have been measured for the first time. They are expected to provide better constraints on some of the higher-order non-perturbative parameters [5]. Figure 1 shows examples of the measured hadron-mass and combined moments.

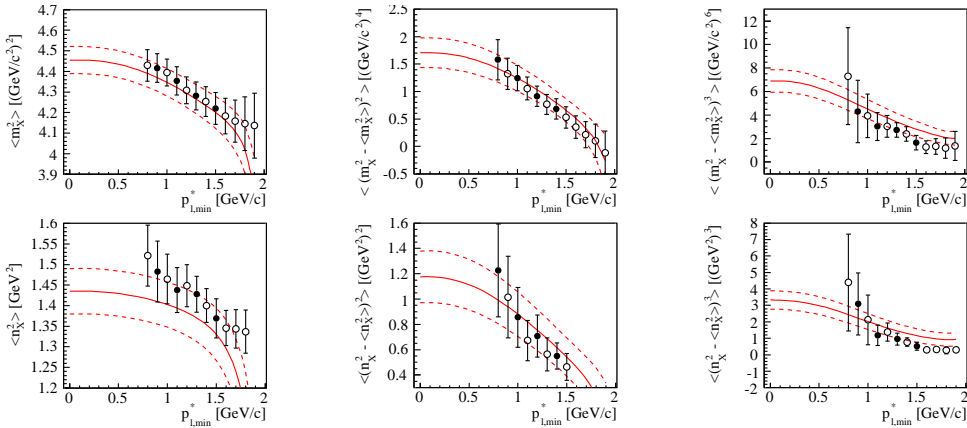


Figure 1: Measured hadron-mass moments, $\langle m_X^n \rangle$, and combined mass-and-energy moments, $\langle n_X^n \rangle$, as a function of the minimum lepton momentum, $p_{\ell, min}^*$, from BaBar [4]. The solid and dashed lines illustrate the OPE fit and its uncertainties, respectively.

Belle has measured electron-energy and hadron-mass moments [6] based on 152×10^6 $B\bar{B}$ pairs. The experimental procedure is similar to the one used in the BaBar analysis. One of the main differences is that detector effects in the measured spectra are removed by using an unfolding method with a detector response matrix obtained from simulation. From the unfolded distributions,

Kinetic scheme	$ V_{cb} $ (10^{-3})	$m_b^{(kin)}$ (GeV)	μ_π^2 (GeV^2)
BaBar ($B \rightarrow X_c \ell \nu + B \rightarrow X_s \gamma$) [4]	41.88 ± 0.81	4.552 ± 0.055	0.471 ± 0.070
Belle ($B \rightarrow X_c \ell \nu + B \rightarrow X_s \gamma$) [6]	41.52 ± 0.90	4.543 ± 0.075	0.539 ± 0.079
Belle ($B \rightarrow X_c \ell \nu$) [6]	41.46 ± 0.99	4.573 ± 0.134	0.523 ± 0.106
Global ($B \rightarrow X_c \ell \nu + B \rightarrow X_s \gamma$) [1]	41.54 ± 0.73	4.620 ± 0.035	0.424 ± 0.042
Global ($B \rightarrow X_c \ell \nu$) [1]	41.31 ± 0.76	4.678 ± 0.051	0.410 ± 0.046
1S scheme	$ V_{cb} $ (10^{-3})	$m_b^{(1S)}$ (GeV)	λ_1 (GeV^2)
Belle ($B \rightarrow X_c \ell \nu + B \rightarrow X_s \gamma$) [6]	41.56 ± 0.68	4.723 ± 0.055	-0.303 ± 0.046
Belle ($B \rightarrow X_c \ell \nu$) [6]	41.55 ± 0.80	4.718 ± 0.119	-0.308 ± 0.092

Table 1: Values of $|V_{cb}|$, m_b , and μ_π^2 (λ_1) obtained from OPE fits to moments from BaBar and Belle. For comparison, the global fit performed by HFAG in the kinetic scheme is also shown.

Belle measures the partial branching fraction, the electron-energy moments $\langle E_e^n \rangle$ ($n = 1, \dots, 4$) for $0.4 < p_{\ell, \min}^* < 2.0$ GeV, and the hadron-mass moments $\langle M_X^{2n} \rangle$ ($n = 1, 2$) for $0.7 < p_{\ell, \min}^* < 1.9$ GeV.

HFAG has performed a global fit [1] of the OPE predictions in the kinetic scheme to the measured moments in $B \rightarrow X_c \ell \nu$ and $B \rightarrow X_s \gamma$ decays to determine $|V_{cb}|$, m_b , and the non-perturbative parameters. It includes m_X , E_ℓ and E_γ moments from BaBar, Belle, CDF, CLEO, and DELPHI (64 moments in total). The results of the global fit are given in Table 1. It yields

$$|V_{cb}| = (41.54 \pm 0.43_{fit} \pm 0.08_{\tau_B} \pm 0.58_{theo}) \times 10^{-3}. \quad (3.2)$$

with a relative precision of 1.7%. The first error is the fit error, the second is due the uncertainty on the B lifetime, and the third is an additional theoretical normalization uncertainty of 1.4% due to uncalculated terms in the total rate. The χ^2/ndf of the fit is $26.4/(64 - 7)$; the low value might indicate that theoretical errors are overestimated or that theoretical correlations are not correctly accounted for. Recently concerns have been raised about the inclusion of $B \rightarrow X_s \gamma$ moments in the fit, since their prediction is not purely based on OPE, but involve non-OPE contributions using a shape function. Table 1 shows the results of the global fit with and without $B \rightarrow X_s \gamma$ moments. In addition, it presents fits from BaBar in the kinetic scheme [4] and from Belle in the kinetic and 1S schemes [6]. As the calculations in the two schemes are independent, testing the consistency of the results in both schemes is an important cross-check. The values of $|V_{cb}|$ in both schemes agree well with each other. The values of m_b (and the non-perturbative parameters) need to be translated from one scheme to the other; after scheme translation they are also in good agreement.

4. Exclusive $B \rightarrow X_c \ell \nu$ Decays and $|V_{cb}|$

Exclusive determinations of $|V_{cb}|$ are based on studies of $B \rightarrow D \ell \nu$ and $B \rightarrow D^* \ell \nu$ decays. The main uncertainties are due to our ignorance of the form factors describing the dynamics of the $B \rightarrow D$ and $B \rightarrow D^*$ transitions. The value of $|V_{cb}|$ can be determined from studies of the differential decay rates as a function of the four-velocity transfer from initial to final state, $w = v_B \cdot v_{D^{(*)}}$, where v_B and $v_{D^{(*)}}$ are the four-velocities of the B and $D^{(*)}$ mesons, respectively:

$$\frac{d\Gamma(B \rightarrow D \ell \nu)}{dw} = \frac{G_F^2}{48\pi^3} |V_{cb}|^2 K_D(w) |G(w)|^2, \quad \frac{d\Gamma(B \rightarrow D^* \ell \nu)}{dw} = \frac{G_F^2}{48\pi^3} |V_{cb}|^2 K_{D^*}(w) |F(w)|^2 \quad (4.1)$$

with phase space factors $K_D(w)$, $K_{D^*}(w)$ and form factors $G(w)$ and $F(w)$. In the limit of infinite heavy-quark masses, Heavy-Quark Symmetry (HQS) predicts that $G(w=1) = 1$ and $F(w=1) = 1$. For finite quark masses, $G(1)$ and $F(1)$ can be calculated with Lattice QCD (LQCD). Experiments measure the product $G(1)|V_{cb}|$ or $F(1)|V_{cb}|$ by fitting the measured $d\Gamma/dw$ distribution and extrapolating to $w = 1$. The parametrization of the form factors [7] depends on one parameter, ρ_D^2 , for $B \rightarrow D\ell\nu$ (pseudoscalar) and three parameters, $\rho_{D^*}^2$, R_1 and R_2 , for $B \rightarrow D^*\ell\nu$ (vector).

Belle has presented preliminary results of an untagged $B \rightarrow D^*\ell\nu$ analysis [8] based on 152×10^6 $B\bar{B}$ pairs. The product $F(1)|V_{cb}|$ and the form-factor parameters are obtained from a fit of the expression for $d\Gamma/dw$ to the distributions of w and three decay angles. The preliminary results are $F(1)|V_{cb}| = (34.3 \pm 0.2 \pm 1.0) \times 10^{-3}$, $\rho_{D^*}^2 = 1.293 \pm 0.045 \pm 0.029$, $R_1 = 1.495 \pm 0.045 \pm 0.029$, $R_2 = 0.844 \pm 0.034 \pm 0.019$, where the first errors are statistical and the second systematic.

BaBar has published a simultaneous measurement of $B \rightarrow D\ell\nu$ and $B \rightarrow D^*\ell\nu$ decays [9] using a novel technique, using 230×10^6 $B\bar{B}$ pairs. In this analysis only the final-state $D\ell$ system ($D^\mp\ell^\pm$ for B^0 decays and $D^0\ell^\pm$ for B^\pm decays) is reconstructed. One advantage of this approach is that it does not depend on the reconstruction of the slow pion from the $D^* \rightarrow D\pi$ decay. The signal and background contributions are estimated in a global fit to three kinematic variables: the momentum of the D meson, p_D^* , and of the charged lepton, p_ℓ^* , in the $Y(4S)$ frame, and the cosine of the angle between the B meson and the $D\ell$ system, $\cos\theta_{D\ell}$. The global fit yields the total branching fractions, $\mathcal{B}(B \rightarrow D\ell\nu) = (2.34 \pm 0.03 \pm 0.13) \times 10^{-2}$, $\mathcal{B}(B \rightarrow D^*\ell\nu) = (5.40 \pm 0.02 \pm 0.21) \times 10^{-2}$, and the form-factor parameters, $\rho_D^2 = 1.20 \pm 0.04 \pm 0.07$ and $\rho_{D^*}^2 = 1.22 \pm 0.02 \pm 0.07$. These results can be translated to $G(1)|V_{cb}| = (43.1 \pm 0.8 \pm 2.3) \times 10^{-3}$ and $F(1)|V_{cb}| = (35.9 \pm 0.2 \pm 1.2) \times 10^{-3}$.

In addition to the untagged analysis, BaBar has performed a hadronic-tag measurement of $B \rightarrow D\ell\nu$ decays [10], based on 460×10^6 $B\bar{B}$ pairs. The selected data samples contain 1108 ± 45 $B^0 \rightarrow D^-\ell^+\nu$ and 2147 ± 69 $B^+ \rightarrow \bar{D}^0\ell^+\nu$ decays. A combined fit to the B^0 and B^+ samples yields $G(1)|V_{cb}| = (43.0 \pm 1.9 \pm 1.4) \times 10^{-3}$ and $\rho_D^2 = 1.20 \pm 0.09 \pm 0.04$. The hadronic-tag analysis has the advantage that backgrounds are strongly reduced and thus depends much less on background uncertainties, which are dominant in the untagged analyses.

Figure 2 shows all measurements of $G(1)|V_{cb}|$ and ρ_D^2 for $B \rightarrow D\ell\nu$ and of $F(1)|V_{cb}|$ and $\rho_{D^*}^2$ for $B \rightarrow D^*\ell\nu$ performed so far, and the current average from HFAG [1]. While the $B \rightarrow D\ell\nu$ measurements are in good agreement with each other ($\chi^2/ndf = 1.3/8$), the agreement between the $B \rightarrow D^*\ell\nu$ measurements is not good ($\chi^2/ndf = 39.6/21$). Together with recent LQCD calculations of $G(1) = 1.074 \pm 0.024$ [11] and $F(1) = 0.921 \pm 0.024$ [12], one obtains

$$|V_{cb}| = (39.4 \pm 1.4 \pm 0.9) \times 10^{-3} \text{ from } B \rightarrow D\ell\nu, \quad (4.2)$$

$$|V_{cb}| = (38.8 \pm 0.5 \pm 1.0) \times 10^{-3} \text{ from } B \rightarrow D^*\ell\nu, \quad (4.3)$$

where the first error is experimental and the second theoretical (form factor). The exclusive and inclusive determinations of $|V_{cb}|$ agree only at the $\sim 2\sigma$ level.

5. Inclusive $B \rightarrow X_u\ell\nu$ Decays and $|V_{ub}|$

For inclusive charmless semileptonic decays, $B \rightarrow X_u\ell\nu$, the total decay rate can be described by the same OPE as for $B \rightarrow X_c\ell\nu$. It is proportional to the product of $|V_{ub}|^2 \cdot m_b^5$ and a function that

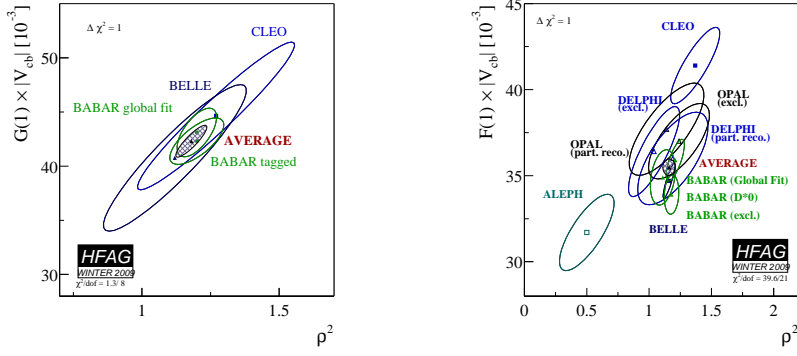


Figure 2: $\Delta\chi^2 = 1$ contours for measurements of $|V_{cb}|$ times form factor and the slope parameter $\rho_{D^{(*)}}$ for $B \rightarrow D\ell\nu$ (left) and $B \rightarrow D^*\ell\nu$ (right) decays. The HFAG average is shown as shaded ellipse.

accounts for electroweak and QCD corrections, and is predicted with a precision of about 5%. The error is dominated by the uncertainty on m_b . The biggest experimental challenge is the suppression of $B \rightarrow X_c\ell\nu$ decays, whose rate exceeds the signal rate by about a factor of 50. For background suppression, the kinematic differences between $B \rightarrow X_u\ell\nu$ and $B \rightarrow X_c\ell\nu$ decays are exploited by applying selection criteria on kinematic variables such as m_X , E_ℓ or q^2 , which results in a strongly reduced measured fraction of the total rate. This phase-space restriction destroys the convergence of the QPE, introducing sensitivity to the effects of Fermi motion of the b -quark inside the B meson. The Fermi motion is inherently non-perturbative and within the OPE it is described by a non-local distribution function, the shape function, which must be measured experimentally. The OPE predicts the first few moments of the shape function, and the shape function can be parameterized in terms of the b -quark mass and non-perturbative parameters obtained from fits to moments of inclusive $B \rightarrow X_c\ell\nu$ or $B \rightarrow X_s\gamma$ spectra (see Section 3).

BaBar has published a hadronic-tag analysis of $B \rightarrow X_u\ell\nu$ decays [13] based on a sample of 383×10^6 $B\bar{B}$ pairs in which the signal is extracted from various kinematic variables. Partial branching fractions, $\Delta\mathcal{B}(B \rightarrow X_u\ell\nu)$, are measured for selection criteria on the hadron mass, m_X , the light-cone momentum of the hadron, $P_+ = E_X - |\vec{p}_X|$, and a combination of cuts on m_X and the four-momentum transfer squared of the semileptonic decay, $q^2 = (p_\ell + p_\nu)^2$. A similar analysis has been performed by Belle [14].

The value of $|V_{ub}|$ can be obtained from the measured partial branching fraction and the partial rate predicted by theory, $\Delta\zeta$, for the analyzed phase space by using the relation $|V_{ub}| = \sqrt{\Delta\mathcal{B}/(\tau_B\Delta\zeta)}$, where τ_B is the average B lifetime. Several theoretical calculations are available: BLNP [15], BLL [16], GGOU [17], DGE [18], ADFR [19]. Table 2 exemplarily presents the $|V_{ub}|$ values obtained for three calculations (BLNP, GGOU and DGE) and the most recent measurements, as compiled by HFAG [1]. The uncertainties are dominated by the theoretical uncertainty on $\Delta\zeta$.

The impact of the uncertainties on the shape function and on m_b can be significantly reduced in measurements that cover a larger portion of the phase space. Belle has recently published an analysis [21] based on 657×10^6 $B\bar{B}$ pairs which covers about 90% of the $B \rightarrow X_u\ell\nu$ phase space and uses a multivariate technique to suppress the $B \rightarrow X_c\ell\nu$ background. Figure 3 shows the measured m_X and q^2 spectra. In this measurement, $|V_{ub}|$ is determined with a relative precision of 7% (see Table 2); the error contributions from theory and m_b amount to only 4%.

Measurement	$ V_{ub} $ (10^{-3})		
	BLNP [15]	GGOU [17]	DGE [16]
BaBar E_e [20]	$4.18 \pm 0.24^{+0.29}_{-0.31}$	$4.05 \pm 0.23^{+0.22}_{-0.32}$	$4.06 \pm 0.27^{+0.27}_{-0.26}$
BaBar m_X [13]	$4.02 \pm 0.19^{+0.27}_{-0.29}$	$3.98 \pm 0.19^{+0.26}_{-0.28}$	$4.23 \pm 0.20^{+0.21}_{-0.16}$
BaBar $m_X - q^2$ [13]	$4.32 \pm 0.28^{+0.29}_{-0.31}$	$4.22 \pm 0.28^{+0.33}_{-0.35}$	$4.26 \pm 0.28^{+0.23}_{-0.19}$
BaBar P_+ [13]	$3.65 \pm 0.24^{+0.25}_{-0.27}$	$3.43 \pm 0.22^{+0.28}_{-0.27}$	$3.70 \pm 0.24^{+0.31}_{-0.24}$
HFAG average [1]	$4.06 \pm 0.15^{+0.25}_{-0.27}$	$4.03 \pm 0.15^{+0.20}_{-0.25}$	$3.70 \pm 0.24^{+0.31}_{-0.24}$
Belle multi-var. [21]	$4.37 \pm 0.26^{+0.23}_{-0.21}$	$4.41 \pm 0.26^{+0.12}_{-0.22}$	$4.46 \pm 0.26^{+0.15}_{-0.16}$

Table 2: Inclusive determinations of $|V_{ub}|$ for various measurements and three theoretical calculations (BLNP, GGOU, DGE). The first error is experimental, the second theoretical and due to m_b .

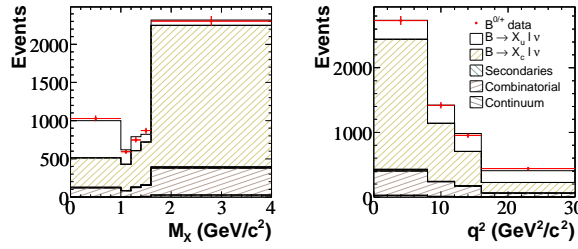


Figure 3: Measured spectra of the hadron mass m_X and the four-momentum transfer squared q^2 for the inclusive $B \rightarrow X_u \ell \nu$ analysis from Belle [21].

6. Exclusive $B \rightarrow X_u \ell \nu$ Decays and $|V_{ub}|$

The $B \rightarrow \pi \ell \nu$ decay is the most promising decay mode for a precise exclusive determination of $|V_{ub}|$, both experimentally and theoretically. The differential decay rate is given by

$$\frac{d\Gamma(B^0 \rightarrow \pi^- \ell^+ \nu)}{dq^2} = \frac{G_F^2}{24\pi^3} P_\pi^3 |V_{ub}|^2 |f_+(q^2)|^2, \quad (6.1)$$

where $f_+(q^2)$ is the $B \rightarrow \pi$ form factor whose normalization must be predicted by theory. A number of $B \rightarrow \pi \ell \nu$ measurements with different tagging techniques exist, but untagged analyses still provide the most precise results. Here the neutrino is inferred from the missing energy and momentum in the event and is then combined with a charged lepton and a pion to form a $B \rightarrow \pi \ell \nu$ candidate. The background in this analysis consists predominantly of $B \rightarrow X_c \ell \nu$ decays, but also $e^+ e^- \rightarrow q\bar{q}$ ($q = u, d, s, c$) events and other $B \rightarrow X_u \ell \nu$ decays contribute.

BaBar has measured the $B^0 \rightarrow \pi^- \ell^+ \nu$ branching fraction and q^2 spectrum [22] with a good accuracy, using $227 \times 10^6 B\bar{B}$ pairs. In this analysis, the signal yields are extracted from a maximum-likelihood fit to the two-dimensional ΔE vs. m_{ES} distribution (see Section 3) of the signal B meson in twelve bins of q^2 . This fit allows for an extraction of the q^2 dependence of the form factor $f_+(q^2)$. As shown in Fig. 4 (left), the shape of the measured spectrum is compatible with the ones predicted by LQCD [23, 24] and light-cone sum rules (LCSR) [25], but incompatible with the ISGW2 quark model [26]. The leading experimental systematic uncertainties are due to neutrino reconstruction and the backgrounds from $e^+ e^- \rightarrow q\bar{q}$ events at low q^2 and from $B \rightarrow X_u \ell \nu$ decays at high q^2 .

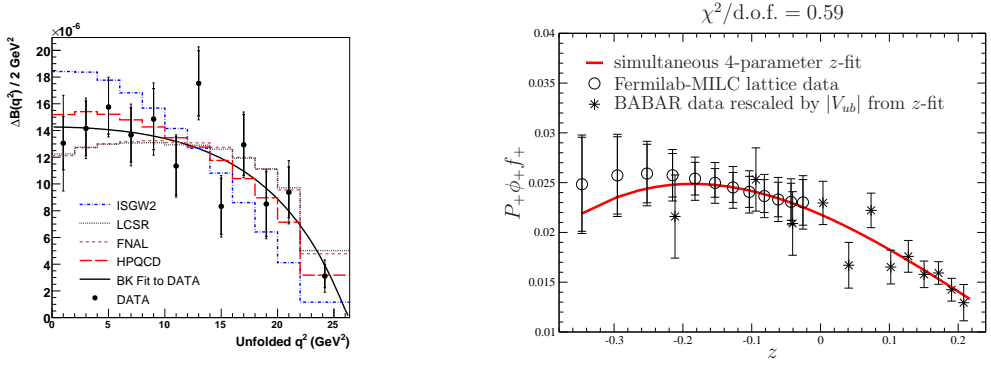


Figure 4: Left: Measured q^2 spectrum from the BaBar untagged $B^0 \rightarrow \pi^- \ell^+ \nu$ analysis [22] compared to theory predictions from LQCD [23, 24], LCSR [25] and the ISGW2 quark model [26]. The line shows a fit of the Becirevic-Kaidalov (BK) form-factor parameterization [27] to the data. Right: Combined fit of the z expansion [28] to BaBar $B^0 \rightarrow \pi^- \ell^+ \nu$ data and FNAL LQCD results [29].

The current world average for the total $B^0 \rightarrow \pi^- \ell^+ \nu$ branching fraction is $(1.36 \pm 0.05 \pm 0.05) \times 10^{-4}$ [1]. The measured partial branching fractions are combined with form-factor calculations from LCSR for $q^2 < 16 \text{ GeV}^2$ and LQCD for $q^2 > 16 \text{ GeV}^2$ to determine $|V_{ub}|$ (see Table 3). The uncertainty on $|V_{ub}|$ is dominated by the theoretical form-factor uncertainty. Neither LQCD nor LCSR calculations predict $f_+(q^2)$ over the full q^2 range. Recently, combined fits to data and LQCD calculations have been performed, which use the so-called z expansion [28] to parameterize $f_+(q^2)$ over the whole q^2 range. These fits make use of the full shape information from data and the normalization and shape information from theory to decrease the uncertainty on $|V_{ub}|$. A z -expansion fit performed by the FNAL group [29] to BaBar data and FNAL/MILC LQCD results yields $|V_{ub}| = (3.38 \pm 0.36) \times 10^{-3}$, with a relative precision of 11%. Inclusive and exclusive $|V_{ub}|$ determinations agree at the $1 - 2\sigma$ level, depending on the choices of theoretical calculations.

Calculation	q^2 range	$ V_{ub} $ (10^{-3})
LCSR [25]	$< 16 \text{ GeV}^2$	$3.34 \pm 0.12^{+0.55}_{-0.37}$
HPQCD [23]	$> 16 \text{ GeV}^2$	$3.40 \pm 0.20^{+0.59}_{-0.39}$
FNAL/MILC [24]	$> 16 \text{ GeV}^2$	$3.62 \pm 0.22^{+0.63}_{-0.41}$

Table 3: HFAG averages for $|V_{ub}|$ from $B \rightarrow \pi \ell \nu$. The errors are experimental and theoretical (form factor).

7. Conclusions

We have presented the status of $|V_{cb}|$ and $|V_{ub}|$ determinations from inclusive and exclusive semileptonic decays. The inclusive measurements still yield the more precise results, but there has been much progress in measurements and theoretical calculations for exclusive decays recently. The current relative precision on $|V_{cb}|$ is 1.7% from inclusive and $\sim 3\%$ from exclusive decays. For $|V_{ub}|$ the relative precisions are $\sim 7\%$ and $\sim 11\%$ for inclusive and exclusive decays, respectively. At present there is still a discrepancy between inclusive and exclusive determinations for both $|V_{cb}|$ and $|V_{ub}|$ at the $\sim 2\sigma$ level and further progress from the experimental side, in particular in the

detailed understanding of backgrounds, but also from theoretical calculations of inclusive rates and of hadronic form factors for exclusive decays is needed.

References

- [1] Heavy Flavor Averaging Group, <http://www.slac.stanford.edu/xorg/hfag/semi/fpcp2009/home.shtml>.
- [2] D. Benson, I. I. Bigi, T. Mannel, N. Uraltsev, Nucl. Phys. **B665**, 367 (2003); P. Gambino, N. Uraltsev, Eur. Phys. J. **C34**, 181 (2004); D. Benson, I. I. Bigi, N. Uraltsev, Nucl. Phys. **B710**, 371 (2005).
- [3] C. W. Bauer, Z. Ligeti, M. Luke, A. V. Manohar and M. Trott, Phys. Rev. **D70**, 094017 (2004).
- [4] B. Aubert *et al.* (BaBar collab.), Phys. Rev. **D81**, 032003 (2010).
- [5] P. Gambino *et al.*, JHEP **09**, 010 (2005).
- [6] C. Schwanda *et al.* (Belle collab.), Phys. Rev. **D75** (2007) 032005; P. Urquijo *et al.* (Belle collab.), Phys. Rev. **D75** (2007) 032001; C. Schwanda *et al.* (Belle collab.), Phys. Rev. **D78** (2008) 032016.
- [7] I. Caprini, L. Lellouch and M. Neubert, Nucl. Phys. **B530**, 153 (1998).
- [8] I. Adachi *et al.* (Belle collab.), arXiv:0810.1657 [hep-ex].
- [9] B. Aubert *et al.* (BaBar collab.), Phys. Rev. **D79**, 012002 (2009).
- [10] B. Aubert *et al.* (BaBar collab.), Phys. Rev. Lett. **104**, 011802 (2010).
- [11] M. Okamoto *et al.*, Nucl. Phys. Proc. Suppl. **140**, 461 (2005).
- [12] J. Laiho *et al.*, arXiv:0808.2519 [hep-lat].
- [13] B. Aubert *et al.* (BaBar collab.), Phys. Rev. Lett. **100**, 171802 (2008).
- [14] I. Bizjak *et al.* (Belle collab.), Phys. Rev. Lett. **95**, 241801, 2005.
- [15] B. O. Lange, M. Neubert and G. Paz, Phys. Rev. **D72**, 073006 (2005).
- [16] C. W. Bauer, Z. Ligeti and M. E. Luke, Phys. Rev. **D64**, 113004 (2001).
- [17] P. Gambino, P. Giordano, G. Ossola, N. Uraltsev, JHEP **0710**, 058 (2007).
- [18] J. R. Andersen and E. Gardi, JHEP **0601**, 097 (2006) and update in arXiv:0806.4524 [hep-ph].
- [19] U. Aglietti, F. Di Lodovico, G. Ferrera and G. Ricciardi, Eur. Phys. J. **C59**, 831-840 (2009).
- [20] B. Aubert *et al.* (Belle collab.), Phys. Rev. **D73**, 012006 (2006).
- [21] P. Urquijo *et al.*, Phys. Rev. Lett. **104**, 021801 (2010).
- [22] B. Aubert *et al.*, Phys. Rev. Lett. **98**, 091801 (2007).
- [23] E. Gulez *et al.*, Phys. Rev. **D73**, 074502 (2006); Erratum-ibid. **D75**, 119906 (2007).
- [24] M. Okamoto *et al.*, Nucl. Phys. Proc. Suppl. **140**, 461-463 (2005).
- [25] P. Ball and R. Zwicky, Phys. Rev. **D71**, 014015 (2005).
- [26] D. Scora and N. Isgur, Phys. Rev. **D52**, 2783 (1995).
- [27] D. Becirevic and A. B. Kaidalov, Phys. Lett. **B478**, 417 (2000).
- [28] C. G. Boyd, B. Grinstein and R. F. Lebed, Phys. Rev. Lett. **74**, 4603 (1995); C. G. Boyd and M. J. Savage, Phys. Rev. **D56**, 303 (1997); T. Becher and R. J. Hill, Phys. Lett. **B633**, 61 (2006).
- [29] J. A. Bailey *et al.*, Phys. Rev. **D79**, 054507.